JOURNAL OF GUIDANCE, CONTROL, AND DYNAMICS
Vol. 25, No. 3, May–June 2002

Anatomy of the Constant Radial Thrust Problem

Maruthi R. Akella* and Roger A. Broucke†
University of Texas at Austin, Austin, Texas 78712

The general types of solutions of the low-thrust problem with constant outward radial acceleration are described. We do not use the known closed-form analytical solution in terms of the elliptic integrals because of the lack of physical insight obtained from these mathematical functions. Instead, we use numerical integrations and concepts that are commonly used for nonintegrable dynamic systems, such as the theory of periodic orbits and Poincaré's characteristic exponents.

Introduction

IN this paper, we intend to investigate the solution manifold for a fairly well know low-thrust problem, the constant outward radial acceleration. The trajectories are always planar because the acceleration is permanently in the plane of the orbit. Therefore, we treat it as a two-degree-of-freedom problem. The problem is known to have a closed-form analytical solution, and, therefore, a good number of its properties are already evident.[1–4] The analytical solution can be expressed in terms of the standard elliptic integrals that actually do not give too much insight into their basic properties.

To gain more insight into these properties, our present investigation will have recourse to some methods that are usually employed in classical mechanics and celestial mechanics, such as the boundaries imposed by the potential function, as well as the two integrals of the problem, the energy and the angular momentum. These concepts already allow us to distinguish between the escape trajectories and the bounded trajectories. The use of the effective potential, as well as the value of the energy constant, allows us to define forbidden, as well as allowable, regions of motion. Note that the concept of an effective potential energy has been well employed earlier by Prussing and Coverstone-Carroll[5] in a similar context, but their initial conditions are restricted to that of a circular orbit.

In this paper, we mostly make use of some methods that are commonplace in nonintegrable dynamic systems, such as the restricted three-body problem. In particular, we use numerical integrations to find and classify periodic orbits, and we use Poincaré's characteristic exponents to determine their stability, as well as the bifurcations between different types of orbits. This approach allows us to classify the bounded solutions in two basic types, the circular orbits and the annular orbits that bifurcate out of the circular orbits and wrap around them. The analytical properties (such as velocity, energy, etc.) of the circular orbits can be established by simple elementary formulas. On the other hand, the annular orbits are always bounded, enclosed in between and tangent to two concentric circles.

The origin and properties of the annular orbits (number of loops, for instance) can be predicted through the linearization and stability analysis of the circular orbits. To make a manageable classification of the complete set of solutions of the problem (without any loss of generality), we introduce a few simplifying assumptions. First, we introduce a well-defined system of canonical units, so that the number of free parameters is reduced to a minimum. Second, we assume that all solutions possess (at least) one point with minimum value of the radius (and, thus, also $\dot{r} = 0$). We assume that this point occurs at $t = 0$, and we rotate the coordinate axes so that it always lies on the x axis. This basically means that, initially, we always have $\dot{r} = \theta = 0$. The only initial values to be varied and explored are, thus, r and $\dot{\theta}$ or, equivalently, x and $\dot{y}$.

All analytical results have been verified as much as possible with numerical integrations. In particular, we have also used the method of Poincaré surfaces of section (at constant energy levels) to verify the global classification of all of the possible solutions. The idea consists of plotting discrete points $\dot{r}$ vs r each time the orbit crosses the x axis.

On these surfaces of section, the circular solutions appear as fixed points, with constant r and $\dot{r} = 0$. Actually, we find both elliptic as well as hyperbolic fixed points, corresponding to stable and unstable circular orbits.

Equations of Motion

The problem we intend to study here, the constant acceleration radial thrust problem, is a two-degree-of-freedom dynamic system because the force is permanently in the plane of the position and velocity vectors. It can be defined by the conservative Lagrangian in polar coordinates r and θ:

$$L = \tfrac{1}{2}(\dot{r}^2 + r^2\dot{\theta}^2) + \mu/r + a_T r \tag{1}$$

Here $\mu = GM$ is the gravitation constant and a_T is the magnitude of the constant radial acceleration. The potential function $\mu/r + a_T r$ consists of two terms, the gravitational central force term and the second term, which is the radial-thrust term, usually considered a small perturbation. We will assume $a_T > 0$, so that we have an outward radial thrust. The Lagrangian in Eq. (1) is obtained by taking the difference between kinetic energy function T and the potential energy V, as defined by

$$T = \tfrac{1}{2}(\dot{r}^2 + r^2\dot{\theta}^2) \tag{2}$$

$$V = -\mu/r - a_T r, \qquad V = V(r) \tag{3}$$

The equations of motion derived from the Lagrangian in Eq. (1) are of the usual form

$$\ddot{r} = r\dot{\theta}^2 - \frac{\partial V}{\partial r} = r\dot{\theta}^2 - \frac{\mu}{r^2} + a_T \tag{4}$$

$$\frac{\mathrm{d}}{\mathrm{d}t}(r^2\dot{\theta}) = 0 \tag{5}$$

The radial equation [Eq. (4)] shows that the two forces involved are in opposite directions. We also note that the gravitation force decreases when r increases, so that at some large distance, the radial thrust a_T may actually be larger in magnitude than the gravitational term.

We want to make a few comments here on the possibility of making a complete classification of the totality of solutions of the constant radial acceleration problem. We will first examine the question of units. The equations of motion of the problem contain two constant parameters, $\mu = GM$ and the thrust constant a_T. The constant GM has the dimensions L^3T^{-2} (usually kilometers cubed per

Received 24 April 2001; revision received 27 September 2001; accepted for publication 6 December 2001.

*Assistant Professor, Department of Aerospace Engineering and Engineering Mechanics; makella@mail.utexas.edu. Member AIAA.

†Professor Emeritus, Department of Aerospace Engineering and Engineering Mechanics; broucke@uts.cc.utexas.edu. Senior Member AIAA.

seconds squared in most space applications) whereas a_T is an acceleration, with dimensions LT^{-2}. There are, thus, no masses involved in the problem, only lengths and times. Therefore, we are free to chooses the units of length and time in such a way that μ and a_T take on any arbitrary preassigned value. This will only change the scale of the values and the timing of the evolution, not the intrinsic properties of the solutions of the problem. For this reason, we have made the most of our numerical calculations with the values $\mu = 1.0$ and $a_T = 0.1$, without any loss of generality.

Because Eq. (1) defines a conservative central force, the problem will have two independent first integrals. The first of these is the energy integral:

$$E = T + V = \tfrac{1}{2}(\dot{r}^2 + r^2\dot{\theta}^2) - \mu/r - a_T r = \text{const} \tag{6}$$

The second integral is, of course, the angular momentum integral derived from Eq. (5), corresponding to the angle θ being an ignorable (cyclic) variable:

$$r^2\dot{\theta} = C = \text{const} \tag{7}$$

The quantities E and C are both constants of integration that can be determined with the initial conditions of any orbit. In fact, we could also use the two integrals E and C as the initial values. If the initial conditions are expressed in rectangular coordinates, then they may be written as $(x_0, y_0, \dot{x}_0, \dot{y}_0)$. However, because there are only two free parameters, E and C, we may subject the axes to an arbitrary rotation, and we may select the origin of time in any arbitrary manner. Therefore, we may restrict all initial values by the conditions $y_0 = 0$ and $\dot{x}_0 = 0$. This only means that all of the solutions we examine begin on the x axis and perpendicular to it. We assume, thus, that all solutions have a close approach point where $\dot{r} = 0$. We exclude rectilinear orbits here.

If this is accepted, all solutions of the problem depend on two initial parameters only, which could be x_0 and $\dot{y}_0$ in rectangular coordinates or r_0 and $r_0\dot{\theta}_0$ in polar coordinates. There is also no loss of generality in assuming that x_0 and $\dot{y}_0$ are always positive. However, there may be some slight sign of ambiguities in converting E and C to x_0 and $\dot{y}_0$, for instance. If we consider only direct orbits, then the equations giving E and C are

$$E = \tfrac{1}{2}\dot{y}_0^2 - \mu/x_0 - a_T x_0 \tag{8}$$

$$C = x_0\dot{y}_0 > 0 \tag{9}$$

Eliminating $\dot{y}_0 = C/x_0$ between these two equations gives us

$$a_T x_0^3 + E x_0^2 + \mu x_0 - \tfrac{1}{2}C^2 = 0 \tag{10}$$

which is the fundamental cubic of the radial thrust problem. We will provide an elaborate discussion on the fundamental cubic in the following sections.

Effective Potential and Investigation of Motion

The angular momentum integral Eq. (7) is all that is needed to reduce the original system from two to one degree of freedom (also refer to Arnold[5] and Prussing and Coverstone-Carroll[3]), with the following equation of motion and energy integral:

$$\ddot{r} = C^2/r^3 - \mu/r + a_T \tag{11}$$

$$E = \dot{r}^2/2 + C^2/2r^2 - \mu/r - a_T r \tag{12}$$

The first term $r\dot{\theta}^2 = C^2/r^3$ in the radial equation [Eq. (4)] is well known to be the centrifugal acceleration.

Our problem is equivalent to the one-dimensional motion of a unit point mass in the central force field subject to radial thrust acceleration, described by

$$\ddot{r} = -\frac{\partial V_{\text{eff}}}{\partial r}, \qquad V_{\text{eff}} = V_{\text{eff}}(r) = V(r) + \frac{C^2}{2r^2} \tag{13}$$

The quantity $V_{\text{eff}}(r)$ is called the effective potential energy. It is easy to see from Eqs. (6) and (13) that the total energy in the equivalent one-dimensional problem,

$$E_1 = \tfrac{1}{2}\dot{r}^2 + V_{\text{eff}}(r) \tag{14}$$

is the same as the total energy in the original two-dimensional problem, $E = T + V$.

We can fix the value of the angular momentum C and determine the qualitative shape/behavior of $V_{\text{eff}}(r)$ with respect to r. Before doing so, we present the following remarks:

1) Let us look at the case $\lim_{r\to 0} V_{\text{eff}}(r)$. From the definition of the effective potential in Eq. (13),

$$\lim_{r\to 0} V_{\text{eff}}(r) = \lim_{r\to 0}\left[\underbrace{-\mu/r - a_T r}_{V(r)} + (C^2/2r^2)\right] = +\infty \tag{15}$$

because as $r \to 0$, $|-\mu/r - a_T r|$ can never grow faster than $C^2/(2r^2)$. Thus, the particle cannot fall into the center of the field.

2) For the case $r \to \infty$, we have

$$\lim_{r\to\infty} V_{\text{eff}}(r) = \lim_{r\to\infty}[-\mu/r - a_T r + (C^2/2r^2)] = -\infty$$

because $a_T > 0$.

3) To find the value of $r = r^*$ such that $V_{\text{eff}}(r^*) = 0$, from Eq. (13), we set

$$V_{\text{eff}}(r) = -\mu/r - a_T r + C^2/2r^2 = 0 \tag{16}$$

Because $r = 0$ is not a root of $V_{\text{eff}}(r) = 0$, we rewrite Eq. (16) as a cubic equation in variable r as follows:

$$r^3 + (\mu/a_T)r - C^2/2a_T = 0 \tag{17}$$

such that $r = r^*$ are the roots of this cubic equation. By the use of Vieta substitution for solution of a cubic equation, it is straightforward to establish that Eq. (17) has only one real root and two complex (conjugate) roots. Furthermore, the only real root $r = r^*$ is positive and given by

$$r^* = \left[R^* + \sqrt{R^{*2} + Q^{*2}}\right]^{\frac{1}{3}} + \left[R^* - \sqrt{R^{*2} + Q^{*2}}\right]^{\frac{1}{3}} \tag{18}$$

where

$$R^* = C^2/4a_T, \qquad Q^* = \mu/3a_T$$

4) Next, we consider $\mathrm{d}V_{\text{eff}}/\mathrm{d}r = 0$, to investigate the extremum points of the effective potential. These points would also indicate existence and location of circular orbits. Setting $\mathrm{d}V_{\text{eff}}/\mathrm{d}r = 0$ gives rise to yet another cubic equation

$$r^3 - (\mu/a_T)r + C^2/a_T = 0 \tag{19}$$

Before we solve this cubic, note the difference from the earlier cubic in Eq. (17) that we obtained earlier while solving $V_{\text{eff}}(r) = 0$. The difference between these two cubic equations is subtle yet crucial. The nature of the roots of Eq. (19) is essentially determined by the value of

$$D = \frac{C^4}{4a_T^2} - \frac{\mu^3}{27a_T^3} \begin{cases} > 0 & \text{one real root, two complex roots} \\ = 0 & \text{all real roots, at least two are equal} \\ < 0 & \text{all real and distinct roots} \end{cases} \tag{20}$$

For the case when $D = 0$, it can be shown that two roots r_1 and r_3 of Eq. (19) are equal such that $r_1 = r_3 = \sqrt{[\mu/(3a_T)]}$, and the third root r_2 is given by $r_2 = -2\sqrt{[\mu/(3a_T)]}$. Thus, r_2 is negative and has no physical meaning. On the other hand, when $D > 0$, there exists only one real root that is positive and the other two roots for the cubic equation (19) are complex. We designate the only real root by r_1.

To investigate the nature of the orbits, let us fix the value of angular momentum at any constant value C. The variation of position r with time is easy to visualize by drawing the effective potential energy $V_{\text{eff}}(r)$. For the case $D \geq 0$, we show this variation in Fig. 1.

Let E be the value of the total energy. All orbits corresponding to the given E and C lie in the region $V_{\text{eff}}(r) \leq E$. From Eq. (14), $\dot{r} = 0$ on the boundary of this region, $V_{\text{eff}} = E$. Therefore, the velocity of the mass point, in general, is not equal to zero because $\dot{\theta} \neq 0$ for

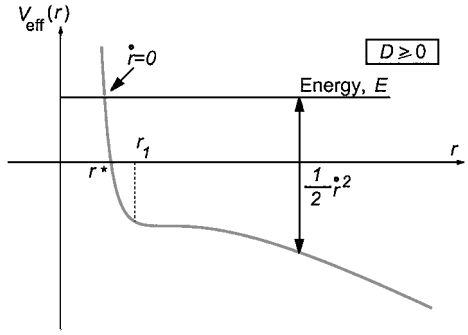

Fig. 1 Effective potential $V_{\text{eff}}(r)$ with respect to radial position r for the case $D \geq 0$ with parameters $\mu = 1.0$ and $a_T = 0.1$; angular momentum C is fixed.

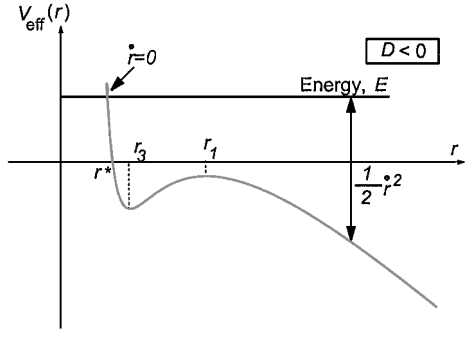

Fig. 2 Effective potential $V_{\text{eff}}(r)$ with respect to radial position r for the case $D < 0$ with parameters $\mu = 1.0$ and $a_T = 0.1$; angular momentum C is fixed.

$C \neq 0$. It is obvious from Fig. 1 that, for $D \geq 0$, irrespective of the value of energy E, all orbits escape. On the boundary $V_{\text{eff}} = E$, if the initial condition $r(0) = r_0$ exactly equals the value of r_1, then we have a circular orbit such that $r(t) = r_1$ for all $t \geq 0$.

In contrast, when we consider the case $D < 0$, the three roots of Eq. (19) are all real and given by

$$r_1 = 2\sqrt{\mu/3a_T}\cos(\Phi/3), \qquad r_2 = 2\sqrt{\mu/3a_T}\cos[(\Phi + 2\pi)/3]$$

$$r_3 = 2\sqrt{\mu/3a_T}\cos[(\Phi + 4\pi)/3]$$

where the angle Φ is given by

$$\Phi = \cos^{-1}\left(\frac{-3C^2\sqrt{3a_T}}{2\mu^{\frac{3}{2}}}\right), \qquad \text{for} \qquad D < 0,\ \Phi \in \left(\frac{\pi}{2}, \pi\right)$$

Because Φ belongs to the second quadrant, it is easy to establish that r_1 and r_3 are positive, whereas $r_2 < 0$. Furthermore, we also obtain the following inequality:

$$0 < r_3 < \sqrt{\mu/3a_T} < r_1$$

This is a really interesting property, as we will later show while discussing the stability of circular orbits. Thus, we obtain a different type of variation for the effective potential $V_{\text{eff}}(r)$ with respect to r in the case $D < 0$. This case is shown in Fig. 2.

Careful inspection of Fig. 2 helps us conclude the following:

1) If the energy E is such that $E < V(r_3)$ or $E > V(r_1)$, all orbits will escape.

2) For $V(r_3) \leq E \leq V(r_1)$, we have either annular or escape orbits depending on the value of r_0. To be more precise, if $r_0 < r_1$, the inequality $V(r_3) \leq E \leq V(r_1)$ gives one or several annular regions in the plane. The other case, when $r_0 > r_1$, leads to escape orbits. In the special case $E = V(r_1)$, with an initial condition $r_0 = r_1$, we have a circular orbit such that $r(t) = r_1$ for all $t \geq 0$. There is a circular orbit when $r_0 = r_3$, as well in the case $E = V_{\text{eff}}(r_3)$.

Allowable Regions of Motion, Based on the Energy Integral

We conclude immediately from the energy equation Eq. (6) that the motion will only be possible for the values of r defined by $r > 0$ and

$$\mu/r + a_T r + E \geq 0 \tag{21}$$

This inequality defines the annular regions of the plane where the motion is possible or not, according to the value of the energy E. It is equivalent to

$$a_T r^2 + Er + \mu \geq 0 \tag{22}$$

which is, of course, a second-degree equation with roots,

$$(r_1, r_2) = \frac{-E \pm \sqrt{E^2 - 4a_T\mu}}{2a_T} \tag{23}$$

Consequently, we will have to discuss the types of roots. More precisely, we will consider the special values $\pm 2\sqrt{(a_T\mu)}$ of the energy because if $E^2 > 4a_T\mu$, we have two distinct real roots (of the same sign).

It is possible to obtain improved regions of motion based on the energy from Eq. (12), by expressing that $\dot{r}^2$ is nonnegative:

$$\dot{r}^2/2 = E - [C^2/2r^2 - \mu/r - a_T r] \geq 0 \tag{24}$$

which is equivalent to a cubic equation,

$$f(r) \triangleq \tfrac{1}{2}r^2\dot{r}^2 = a_T r^3 + Er^2 + \mu r - C^2/2 \geq 0 \tag{25}$$

which is, again, the fundamental cubic of the constant radial thrust problem [see also Eq. (10)]. It is different from the other two cubic equations given in Eqs. (17) and (19). Without going in the detailed discussion of the roots, we may say that the curve $f(r)$ is generally as shown in Fig. 3. However, we will need to discuss the types of roots for the fundamental cubic in more detail. We will use the discriminant Q of the cubic equation (25), as obtained through the standard rules of the Vieta formulas:

$$A = \mu/a_T - E^2/3a_T^2$$

$$B = 2E^3/27a_T^3 - C^2/2a_T - \mu E/3a_T^2$$

$$Q = (B/2)^2 + (A/3)^3$$

Basically, when $Q < 0$, we have three real roots, and when $Q > 0$, there is only one real root. The motion is only possible for the values of r, such that $f(r) > 0$ in Fig. 3, in other words, the regions where $f(r)$ is above the x axis.

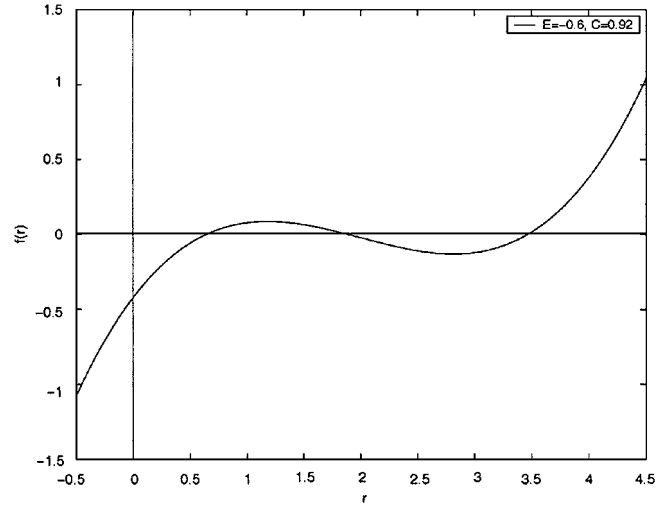

Fig. 3 Illustration of the fundamental cubic for the radial thrust problem with parameters $E = -0.6$ and $C = 0.92$.

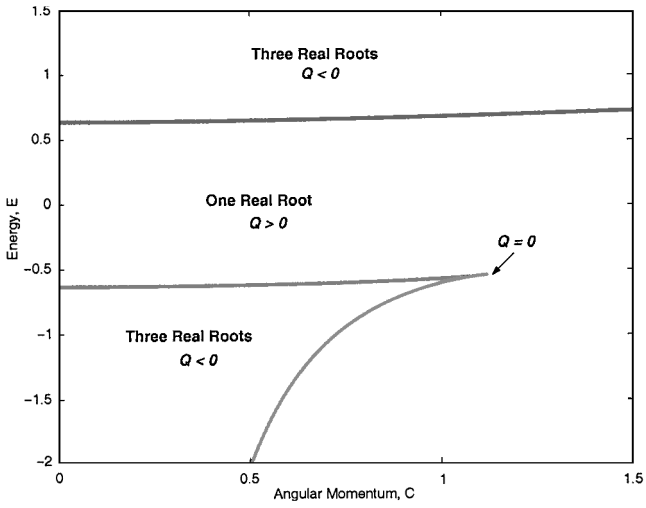

Fig. 4 Roots of the fundamental cubic for the radial thrust problem with $a_T = 0.1$ and $\mu = 1.0$.

The discussion can be further facilitated if we observe that the cubic Eq. (25) depends on two variable parameters, E and C. We will, thus, present Fig. 4, which summarizes the results in the (C, E)-plane (E being the vertical axis).

In Fig. 4, the regions corresponding to three real roots and one real root for the cubic equation are clearly marked. The sharp corner in Fig. 4 corresponds to the critical value $Q = 0$. This is the case of three real and equal roots of the cubic equation (25). It can further be shown that each of these roots equal $r = \sqrt{[\mu/(3a_T)]}$, which can be verified by substituting back in Eq. (25). In the case of three real roots, we usually have only two orbits: the largest root gives an escaping orbit in the outer allowable region, whereas the two other roots correspond to the perigee and apogee of an annular orbit in the inner allowable region.

Circular Orbits

We will now show that the present dynamic system actually admits circular orbits. The two conditions for the existence of circular orbits are, of course, $\dot{r} = 0$ and $\ddot{r} = 0$, and Eqs. (11) and (12) allow us to write them in a more explicit form

$$C^2/r^3 - \mu/r^2 + a_T = 0 \tag{26}$$

$$C^2/2r^2 - \mu/r - a_T r = E \tag{27}$$

These are basically two equations in three unknowns, E, C, and r (the radius of the circular orbit). In principle, we can, thus, solve for any two variables in terms of the third one, so that we may expect a one-parameter family of circular orbits. We will begin with eliminating the quantity C^2/r^2 from Eqs. (26) and (27) to get a single relation between E and r:

$$3a_T r^2 + 2Er + \mu = 0 \tag{28}$$

This is, of course, a quadratic equation in r, which suggests that, for a given value of the energy E, there may be two circular orbits:

$$(r_1, r_2) = \frac{-E \pm \sqrt{E^2 - 3\mu a_T}}{3a_T} \tag{29}$$

if we have the following condition

$$E^2 \geq 3\mu a_T \tag{30}$$

Actually, Eq. (29) clearly shows that for positive E, r_1 and r_2 would both be negative. Thus, the circular orbits can only exist for energies E less than $-\sqrt{(3\mu a_T)}$.

Going back now to Eq. (26) gives us the following equation for the angular momentum, which is clearly the well-known Keplerian formula, but with an additional term due to the thrust:

$$C^2 = \mu r - a_T r^3 \geq 0 \tag{31}$$

Actually, it is also interesting to obtain the constant angular velocity $\dot{\theta} = \omega = C/r^2$ [by manipulating Eq. (31)]:

$$\omega^2 r^3 = \mu - a_T r^2 \tag{32}$$

We recognize here Kepler's third law, $\omega^2 r^3 = \mu$, of the two-body problem, but there is an additional term showing how the radial thrust acceleration a_T affects the period of the circular orbits (see Prussing and Coverstone-Carroll[8]). It is equally interesting to look at the new equation for the linear velocity $v = \omega r$ (which is $v^2 = \mu/r$ in the two-body problem). We obtain from Eq. (32)

$$v = \omega r = \sqrt{\mu/r - a_T r} \tag{33}$$

We again recognize the additional term caused by the radial thrust.

For a given negative value of the energy, there could be either one or two circular orbits. The condition for having two circular orbits is rather complicated:

$$\mu\left[\frac{-E + \sqrt{E^2 - 3\mu a_T}}{3a_T}\right] - a_T\left[\frac{-E - \sqrt{E^2 - 3\mu a_T}}{3a_T}\right]^3 > 0 \tag{34}$$

The qualitative properties and stability of these two circular orbits will be discussed in the sequel.

Poincaré Surfaces of Section

We outline a procedure to compute Poincaré surfaces of section in the constant radial thrust problem. Each Poincaré surface could represent several orbits, all of which correspond to the same constant value of the energy E. The initial conditions are all of the form

$$(x_0, y_0 = 0, \dot{x}_0 = 0, \dot{y}_0)$$

The value of x_0 can be varied to get several orbits on each Poincaré section. Given x_0, the value of $\dot{y}_0$ (>0.0) can be computed from the energy equation (6). At each revolution, a single dot $(x, \dot{x})$ is plotted, corresponding to $y = 0$ and $\dot{y} > 0.0$. In other words, we plot the ascending intersections with the y plane in the space $(x, \dot{x}, y)$.

It is well known that we then have an area-preserving transformation of the $(x, \dot{x})$ plane, or, in other words, a canonical transformation. Fixed points on a Poincaré surface of section correspond to periodic orbits of the dynamic system.

Figure 5 shows a typical Poincaré section with about 20 orbits, all with the same energy value, $E = -0.6$. The parameter $\dot{x}_0$ was varied from 0.0 to 2.0 by steps of 0.1. Each oval curve on Fig. 5 corresponds to one trajectory. The trajectories were integrated for about 100–200 revolutions.

Inspection of the several computer plots similar to Fig. 5 shows that each surface of section has basically one fixed point at the center,

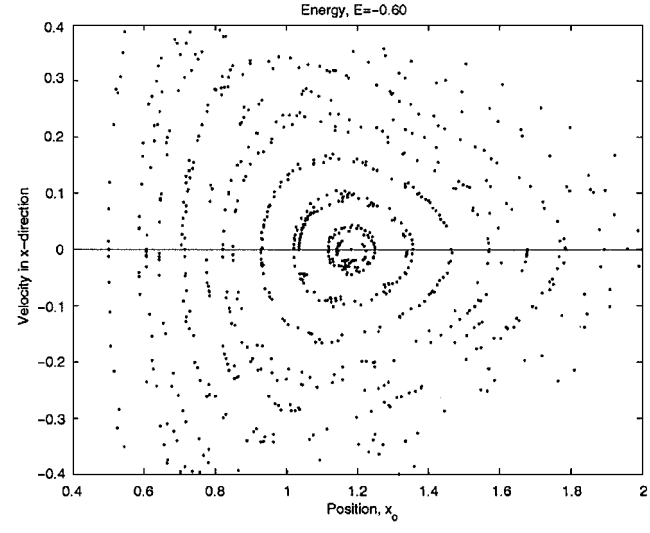

Fig. 5 Poincaré surface of section corresponding to energy $E = -0.60$.

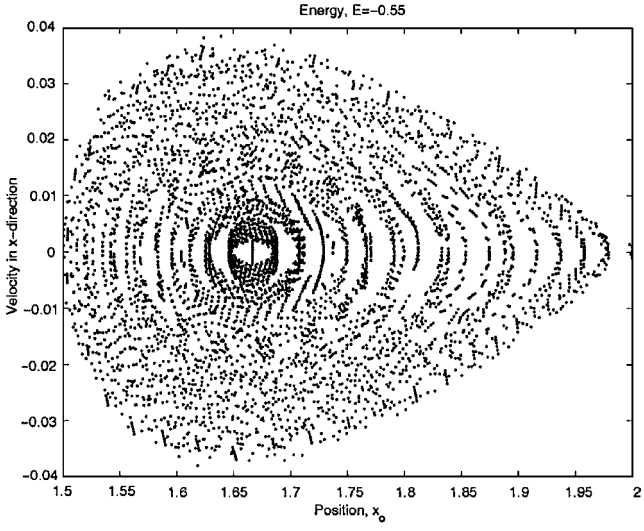

Fig. 6 Poincaré surface of section corresponding to energy $E = -0.55$.

of the elliptic (equal to stable) type, whereas all of the other curves wrap around it. The orbits corresponding to the central fixed point are periodic orbits that close after a single revolution. We verified by numerical integration that they are actually the circular orbits. This shows the extremely important role that is played by these circular orbits: They are the central backbone of the set of annular quasi-periodic orbits that wrap around them on concentric tori in phase space. The fixed point of the circular periodic orbit in Fig. 5 has the numerical values $x_0 = 1.183503419$, $\dot{x}_0 = 0$. The velocity $\dot{y}_0$ is 0.8524075506, and the half-period is equal to 4.361863810. Note that this value of x_0 corresponds to the smaller root r_1 as given by Eq. (29).

We display in Fig. 6 another Poincaré surface of section corresponding to the energy $E = -0.55$. We selected this value because it is so close to the critical value $E = -\sqrt{(3\mu a_T)} = -0.54772255$. Note how small the section is, 1.5–2.0 in the horizontal direction (x_0) with -0.04 to $+0.04$ along the vertical axis ($\dot{x}_0$). There are two fixed points [the two solutions of Eq. (29)]: The stable elliptic point is at $x_0 = 1.66666$, whereas the unstable hyperbolic point is at $x_0 = +2.0$. Both are on the x_0 axis and both correspond to circular orbits, the well-known stable and unstable circular orbits that were described earliear. Figure 6 represents about 35 orbits.

Stability of the Circular Orbits

Given that the dynamics of low radial thrust admit circular orbits, we are interested in investigating the stability of the circular orbits. Danby[6] presents a very nice treatment of this subject in the general framework of analytical dynamics. The stability of the circular orbits can be obtained by studying the equations of motion linearized in the neighborhood of the circular orbit of radius r_0. We replace r by $r_0 + \delta r$ in Eq. (11) for the circular orbit. We first recall from Eq. (32) that the period T_0 and frequency ω_0 of a circular motion are given by the following formulas:

$$\omega_0^2 = \mu/r_0^3 - a_T/r_0, \qquad T_0 = 2\pi/\omega_0 \tag{35}$$

We then make a Taylor series expansion, and we retain only the terms of first order in the small displacement δr. We get a differential equation with constant coefficients, basically a harmonic oscillator:

$$\ddot{\delta} r = -\omega^2 \delta r \tag{36}$$

with the frequency ω defined by

$$\omega^2 = 3C^2/r_0^4 - 2\mu/r_0^3 = \mu/r_0^3 - 3a_T/r_0 = \omega_0^2 - 2a_T/r_0 \tag{37}$$

We need to make the following points:

1) We have a true harmonic oscillator when $\omega^2 > 0$. The circular orbit is considered stable because the displacements δr are sinusoidal in time, with bounded magnitude.

2) We have exponential functions as a solution when $\omega^2 < 0$. The circular orbit is considered unstable because the displacements δr are increasing in time, with unbounded magnitude.

In what follows, we will study the stable case in more detail. First, we can use Eq. (37) to obtain a boundary of the radius of the stable circular orbits:

$$r_0 < \sqrt{\mu/3a_T} \tag{38}$$

This is an expression that was obtained in the earlier sections. If we use the standard values $\mu = 1.0$ and $a_T = 0.1$, we obtain the value $r_0 = \sqrt{(1/0.3)} = 1.825752$.

Knowing that, in general, the stability of orbits gives much information about the dynamic system, we decided to compute the stability of the circular orbits. Another important element in the study of the stability is the fundamental solution matrix $H(t)$ of Eq. (36). This is the matrix whose columns are the two linearly independent solutions of Eq. (36), normalized in such a way that $H(0)$ is the identity matrix:

$$H(t) = \begin{bmatrix} \delta r_1 & \delta r_2 \\ \dot{\delta} r_1 & \dot{\delta} r_2 \end{bmatrix} = \begin{bmatrix} \cos\omega t & (1/\omega)\sin\omega t \\ -\omega \sin\omega t & \cos\omega t \end{bmatrix} \tag{39}$$

We note that the determinant of $H(t)$ is equal to $+1$, at all values of the time t. This matrix is called the state transition matrix. We call the monodromy matrix, the same matrix $H(T_0)$ evaluated at the end of a complete revolution, $t = T_0$, on the nominal circular orbit:

$$H(T_0) = \begin{bmatrix} \cos\omega T_0 & (1/\omega)\sin\omega T_0 \\ -\omega \sin\omega T_0 & \cos\omega T_0 \end{bmatrix} \tag{40}$$

Many rather important properties can be derived from the Monodromy matrix. For instance, the eigenvalues $\lambda_{1,2}$ may be obtained as the roots of the characteristic equation

$$\det \begin{bmatrix} \cos\omega T_0 - \lambda & (1/\omega)\sin\omega T_0 \\ -\omega \sin\omega T_0 & \cos\omega T_0 - \lambda \end{bmatrix} = 0 \tag{41}$$

This characteristic equation finally reduces to the simple form

$$\lambda^2 - 2\lambda \cos\omega T_0 + 1 = 0 \tag{42}$$

We again note that the product of the two roots is $+1$, so that they are reciprocal of one another. This property is a direct consequence of the determinant of $H(t)$ for all values of t being equal to $+1$ from Eq. (39), which we mentioned earlier. The two eigenvalues (λ, λ^{-1}) can be real or complex. If they are real, we have an unstable orbit. If they are complex (in fact, complex conjugates), and on the unit circle, we have a stable orbit. On the other hand, the sum of the two roots is the so-called stability index k and is given by the formula

$$k = \lambda_1 + \lambda_2 = 2\cos\omega T_0 \tag{43}$$

It is rather convenient to base the discussion on the stability index,[7] which is real in both the stable and unstable case.

In the stable case, $k \in [-2, +2]$. The stability boundaries $k = 2$ and -2 play an important role related to bifurcation of orbits, as we will see later.

We computed the stability index of the circular orbits with radius ranging from $r_0 = 1.2$ all the way to the upper boundary of the stable circular orbits $r_0 = \sqrt{[\mu/(3a_T)]} = 1.82574185835$ and show the same variation in Fig. 7.

The boundary between the two classes is the circular orbit at $k = 2$ corresponding to $r_0 = \sqrt{[\mu/(3a_T)]}$. In connection with these developments, $r = \sqrt{[\mu/(3a_T)]}$ is also the circular orbit whose fundamental cubic equation has the triple root. The present value of the radius was also predicted during that discussion.

The main conclusion of the stability calculations is that the inner circular orbits are stable (for $k < 2$), whereas the outer circular orbits are unstable.

The energy E corresponding to any particular circular orbit radius r_0 can be computed by solving Eq. (28) for E. We show a plot of E with respect to this r_0 in Fig. 8.

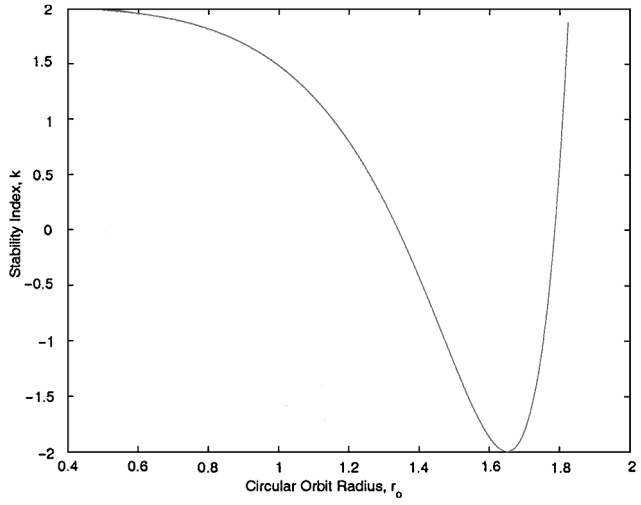

Fig. 7 Stability index k as a function of the circular orbit radius r_0.

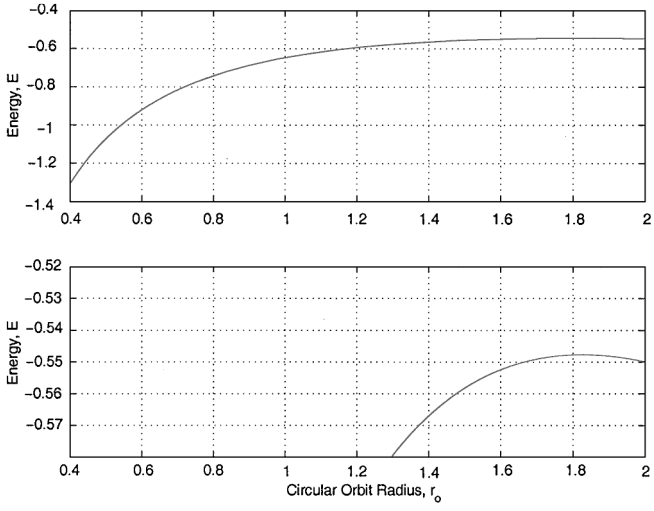

Fig. 8 Stability index k as a function of the circular orbit radius r_0.

Note from Fig. 8 that the variation of E is rather flat with respect to r_0. In fact, it can be seen that the maximum value of energy occurs at the same circular radius that corresponds to the unstable circular orbit with a stability index $k = 2$ (also see Fig. 7). We have there $\omega = \frac{1}{3}$ and $\omega_0 = 0$. This is actually a well-known property in the theory of periodic orbits, as was pointed out by Hénon.[8] In terms of Hénon's classification, we are here in the presence of a type four periodic orbit, which means an orbit with an extremum of the energy, but no new periodic orbits bifurcating out of it. The matrix H in this case is

$$H = \begin{bmatrix} a & b \\ c & d \end{bmatrix} = \begin{bmatrix} +1 & 18.98 \\ 0 & +1 \end{bmatrix}$$

The coefficient b is equal to 18.98, which is the period of that circular orbit. We also see that the coefficient c is zero here. This calculation was done with the original Hénon method,[8] as well as via the Hénon and Guyot method,[9] which requires only a half-revolution integration. The results agree to within six digits. The same result was then also obtained with the use of Hill's equation based on normal and parallel displacements, as described by Deprit and Henrard.[10] This calculation was accurate to about nine digits.

A close inspection of the stability diagram in Fig. 7 also shows that the stable circular orbits are actually divided in two segments by a special orbit with the tangent stability index $k = -2.0$. We are here in the presence of a so-called period doubling phenomenon. In Hénon terminology,[8] we have a periodic orbit of his type five or six. However, because of symmetry of the problem, the stability curve is tangent to the line $k = -2.0$, and we really have a combined type five plus six periodic orbit. The H matrix here is given by

$$H = \begin{bmatrix} a & b \\ c & d \end{bmatrix} = \begin{bmatrix} -1.0 & 0.0 \\ 0.0 & -1.0 \end{bmatrix} \tag{44}$$

We see that the two coefficients b and c are zero. This is the only circular orbit with such a property. The most precise H matrix that we were able to compute was obtained by integrating Hill's equation as described by Deprit and Henrard (see Ref. 10). We show it here to the precision of our calculations:

$$H = \begin{bmatrix} a & b \\ c & d \end{bmatrix} = \begin{bmatrix} -0.99999973 & -0.000214515 \\ 0.000000893 & -0.999999974 \end{bmatrix} \tag{45}$$

with a determinant of 0.999999715 (which should be 1.0). We also verify that $\omega_0 = 0.2$ and $\omega = 0.4$ and that we have exactly $\omega_0/\omega = \frac{1}{2}$. We have, thus, a two to one resonance, also called period doubling in modern dynamics. This special circular orbit is at the origin of a new family of periodic orbits with double period. We will describe it more in detail later.

Annular Orbits and Bifurcations

The general stability theory predicts the birth of new periodic orbits near the stable circular orbits described in the preceding section, through the phenomenon of bifurcation. We will call the new periodic orbits annular orbits. These orbits are always enclosed in between two circular orbits.

Let us assume a stable circular orbit, with a complex eigenvalue for the H matrix, $\lambda = \cos g + i \sin g$ and the other eigenvalue $1/\lambda = \cos g - i \sin g$. The stability index k is then $\lambda + 1/\lambda = 2 \cos g$. The bifurcation to a new periodic orbit with n times as many revolutions happens when the angle g is equal to $2\pi/n$, $(n > 1)$. Let us mention four simple special cases.

Case $n = 2$:

$$g = 180\,\text{deg}, \qquad \cos g = -1.0, \qquad k = -2.0$$

Case $n = 3$:

$$g = 120\,\text{deg}, \qquad \cos g = -\tfrac{1}{2}, \qquad k = -1.0$$

Case $n = 4$:

$$g = 90\,\text{deg}, \qquad \cos g = 0.0, \qquad k = 0.0$$

Case $n = 6$:

$$g = 60\,\text{deg}, \qquad \cos g = \tfrac{1}{2}, \qquad k = 1.0$$

The exact location of the annular orbits with n revolutions can, thus, be predicted by locating the corresponding value of k on the stability diagram in Fig. 7.

The period-doubling case that was mentioned is the simplest situation in this theory. Periodic orbits with two revolutions are supposed to originate near the circular orbit with radius $r_0 = 1.6666667$ where $k = -2.0$ and $\omega/\omega_0 = 2$.

The preceding case can be generalized to the situation where $\omega/\omega_0 = n$, where n is an integer. For instance, when $\omega/\omega_0 = 3$, we have a period-tripling bifurcation with $k = -1$. Also, when $\omega/\omega_0 = 4$, we have a quadruple period bifurcation with $k = 0$.

A closer examination of the stability curve in Fig. 7 reveals many interesting properties related to the bifurcation of certain circular orbits into periodic annular orbits. These bifurcations, in general, occur when the two frequencies ω and ω_0 are commensurable. To have a frequency ratio $\omega/\omega_0 = m/n$, we can combine Eqs. (35) and (37) to obtain the following expression for r_0:

$$r_0 = \sqrt{\frac{(n^2 - m^2)\mu}{(3n^2 - m^2)a_T}} \tag{46}$$

for positive integer values of m and n that are relatively prime. The value of r_0 computed from Eq. (46) establishes the existence of periodic orbits that bifurcate from the circular orbit at

$r = r_0$. For example, when $\omega/\omega_0 = \frac{3}{2}$, we have a bifurcation with $k = 2\cos(4\pi/3) = -1$. Also, when $\omega/\omega_0 = \frac{4}{3}$, we have a bifurcation with $k = 2\cos(3\pi/2) = 0$.

Numerical Experiments with Bifurcation Orbits

We performed numerical experiments for the purpose of discovering some of the annular orbits that are supposed to exist as bifurcations out of circular orbits at specific values of the stability index k. We especially studied two cases in detail: $k = -2$ and -1.

Period Doubling at $k = -2$

We start our calculations from the circular orbit with the following numerical data:

$$x_0 = 1.65144, \qquad \dot{y}_0 = 0.6636174664$$

$$E = -0.5504820708$$

Next, we searched for new periodic orbits in the vicinity, which are not circular and have approximately a double period. Our search software, based on Newton iterations, found the following periodic orbit:

$$x_0 = 1.656097859, \qquad \dot{y}_0 = 0.6617495897$$

$$E = -0.55048258$$

This orbit was then extended, by analytical continuation on the computer, into a family of 100 consecutive periodic orbits. The last one of these orbits is shown in Fig. 9.

The numerical data for the last three periodic orbits obtained from analytical continuation are summarized in Table 1. We also note that the stability index k of all of these orbits is 2.0, (accurate to 10 digits in our calculations).

Periodic Orbits with Triple Period at $k = -1$

Here, we start our calculations from the circular orbit with the following numerical data:

$$x_0 = 1.47450, \qquad \dot{y}_0 = 0.7285231628, \qquad E = -0.56027300 \tag{47}$$

Table 1 Numerical data for three periodic orbits that have a double period

x_0	$\dot{y}_0$	E	k
1.999580388	0.5394789214	−0.5545442104	2.0
2.009580388	0.5362605051	−0.5547866952	2.0
2.019580388	0.5330550445	−0.5550365608	2.0

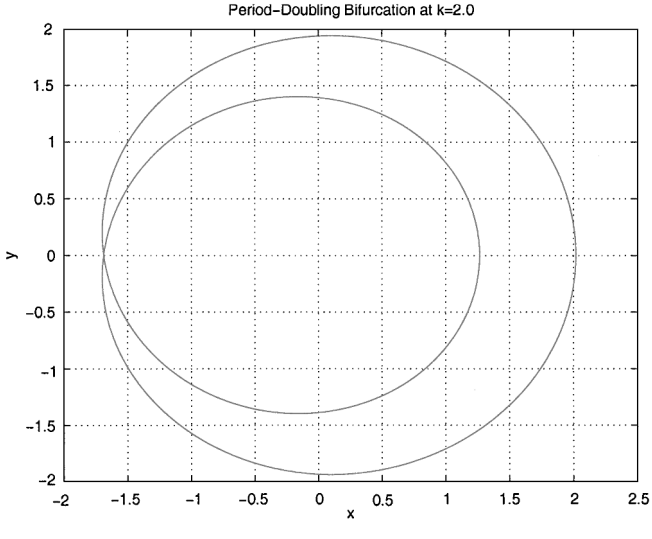

Fig. 9 Annular orbit with a period-doubling bifurcation.

Table 2 Numerical data for two periodic orbits with triple period

x_0	$\dot{y}_0$	E	k
1.469997036	0.7307437522	−0.5602799685	2.0
1.478999369	0.7262957257	−0.5602800066	2.0

Table 3 Numerical data for two periodic orbits that are obtained via analytical continuation starting from a periodic orbit with triple period

x_0	$\dot{y}_0$	E	$T/2$	k
2.002481897	0.5144037108	−0.5673228956	20.76561343	2.0
2.012481897	0.5110079192	−0.5675825226	20.83249195	2.0

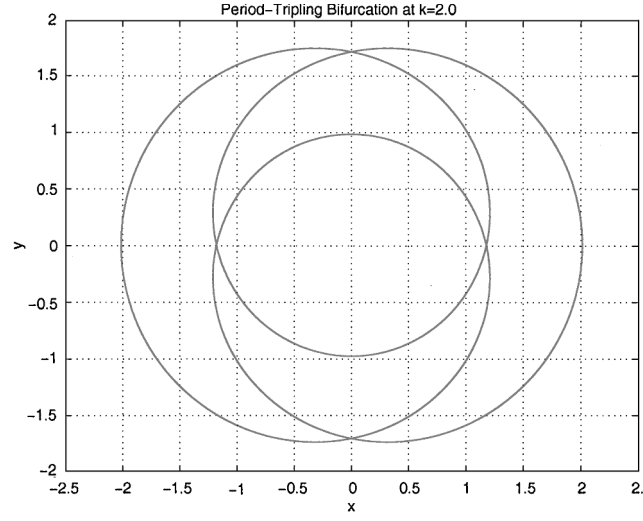

Fig. 10 Annular orbit with a period-tripling bifurcation.

We note that, to the precision of our calculations, the stability index of the preceding orbit is −1.000632195.

Next, we searched for new periodic orbits in the vicinity that are not circular and have approximately a triple period. Our search software found the two following periodic orbits as given in Table 2. One of them starts inside the circular orbit defined by the initial conditions in Eq. (47), whereas the second one starts outside the circular orbit. The second orbit of these two periodic orbits (with triple period) was then extended, by analytical continuation on the computer, into a family of 100 consecutive periodic orbits. The last one of these orbits is shown in Fig. 10. The numerical data for the last two periodic orbits obtained by analytical continuation are given in Table 3. We note again that the stability index of all of these orbits is 2.0 (accurate to at least eight digits in our calculations).

Conclusions

In this paper, we study the dynamics of the constant outward acceleration problem due to radial thrust. This is one of the rare non-Keplerian problems that admit closed-form solutions in terms of elliptic integrals. We establish the regions of allowable motion based on the energy integral, as well as escape conditions for this problem. The existence of circular orbits and their stability is also discussed. Furthermore, we show that the circular orbits bifurcate into a continuous family of periodic annular orbits. Several numerical examples are presented to illustrate the different types of orbits possible in this problem.

References

[1] Tsien, H., "Take-off from Satellite Orbit," *Journal of the American Rocket Society*, Vol. 23, No. 4, 1953, pp. 233–236.

[2] Battin, R. H., *An Introduction to the Mathematics and Methods of Astrodynamics*, AIAA Education Series, AIAA, New York, 1987, pp. 408–415.

[3]Prussing, J. E., and Coverstone-Carroll, V., "Constant Radial Thrust Acceleration Redux," *Journal of Guidance, Control, and Dynamics*, Vol. 21, No. 3, 1998, pp. 516–518.

[4]Akella, M. R., "On Low Radial Thrust Spacecraft Motion," *Journal of Astronautical Sciences* (R. H. Battin special issue), Vol. 48, No. 2–3, 2000, pp. 149–161.

[5]Arnold, V., *Mathematical Methods of Classical Mechanics*, Springer-Verlag, New York, 1989, pp. 33–40.

[6]Danby, J. M. A., *Fundamentals of Celestial Mechanics*, Willman–Bell, Richmond, VA, 1988, p. 59.

[7]Whittakar, E. T., *A Treatise on the Analytical Dynamics*, 4th ed., Cambridge Univ. Press, Cambridge, England, U.K., 1959, p. 404.

[8]Hénon, M., "Exploration Numerique du Probleme Restreint," *Masses Egales, Stabilite des Orbites Periodiques, Extrait des Annales d'Astrophysique*, Vol. 28, No. 6, 1965, pp. 992–1007.

[9]Hénon, M., and Guyot, M., "Stability of Periodic Orbits in the Restricted Problem," *Periodic Orbits, Stability and Resonances*, edited by G. E. O. Giacaglia, Reidel, Dordrecht, The Netherlands, 1970, pp. 349–374.

[10]Deprit, A., and Henrard, J., "Natural Families of Periodic Orbits," *Astronomical Journal*, Vol. 72, No. 1, 1957, pp. 158–172.